Compounds with Intermediate Spin. 9*. Crystal Structure of a Novel Tris(4-morpholinecarbodithiato)iron(III)–Dichloromethane Phase. Correlation between Structural and Magnetic Properties in Tris(4-morpholine-carbodithiato)iron(III) Solvates

KENNY STAHL

Inorganic Chemistry 2, Chemical Center, University of Lund, P.O. Box 740, S-220 07 Lund, Sweden

Received March 29, 1983

The crystal structure of $Fe(S_2CNC_4H_8O)_3 \cdot CH_2Cl_2$ phase III, $M_r = 627.11$, has been determined with direct and Fourier methods from X-ray four-circle single-crystal diffractometer data at 293 K. The space group is triclinic, $P\bar{1}$, with Z = 2; a = 9.264(1) Å; b = 10.459(1) Å; c = 13.665(2) Å; $\alpha = 100.65(1)°$; $\beta = 95.60(1)°$; $\gamma = 105.83(1)°$; V = 1236(1) Å^3; $D_x = 1.684$ g cm^{-3}. The refinement converged to R = 0.028. The effective magnetic moment was determined using the Faraday method and is constant at 5.9 B.M. between 77 and 320 K. The complexes are mononuclear with pseudosymmetry D_3 and van der Waals packed together with disordered dichloromethane molecules. The geometry of the complex is that expected from a high spin tris(dithiocarbamato)-iron(III)compound. The effective magnetic moments of tris(4-morpholinecarbodithiato)iron(III) solvates are found to be strongly correlated to the deformation of the central C–N bond in the ligands. Increased deformation decreases the π-bond overlap and favours the low spin canonical form of the ligand. Non-polar solvents crystallize around the non-polar morpholine ring of the ligand resulting in a stronger deformation of the ligand than for polar solvents crystallizing preferably near the FeS_6 core of the complex.

Introduction

The magnetic properties of substituted tris(dithiocarbamato)iron(III) ($Fe(dtc)_3$) compounds can be described as a thermal equilibrium of the low-spin doublet and the high-spin sextet forms of the com-

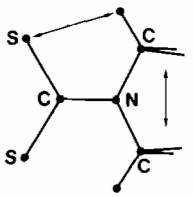

Fig. 1. The steric interaction (indicated by arrows) in a dithiocarbamate ligand.

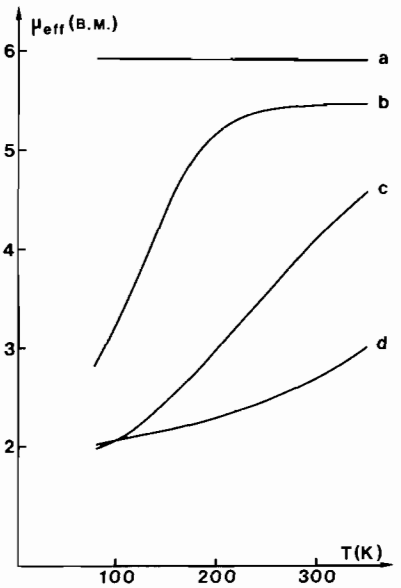

Fig. 2. Effective magnetic moment *vs.* temperature for $Fe(dtc)_3$ compounds with various substituents: *a*. Tetramethylene, *b*. Dibutyl, *c*. Dimethyl, *d*. Diisopropyl.

*For part 8 in this series see Ref. 5.

0020-1693/83/$3.00

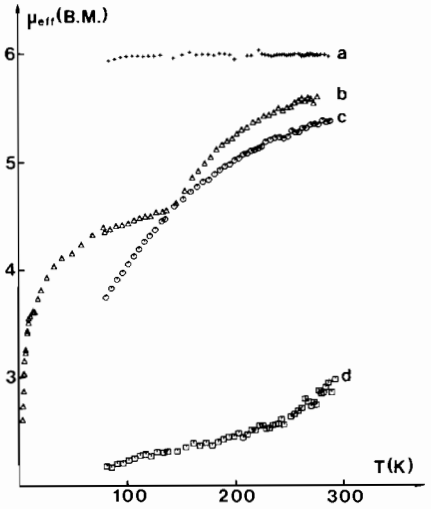

Fig. 3. Effective magnetic moment *vs.* temperature for various tris(4-morpholinecarbodithioato)iron(III) solvates: *a*. CH_2Cl_2 (phase III), *b*. CH_2Cl_2 (phase I and II), *c*. Desolvated *a*, *b*, or *d*, *d*. $2 \cdot C_6H_6$.

plexes [1]. The effective magnetic moment (μ_{eff}) may thus vary between ~2 B.M. (1 B.M. = $9.274 \cdot 10^{-24}$ J T^{-1}) and 5.92 B.M. The actual μ_{eff} *vs.* T behaviour has been shown to be strongly dependent on the substituents of the ligand [2]. The substituents interfere sterically with the S-atoms and thereby influence the ligand bite (Fig. 1). The most bulky substitutents *e.g.* isopropyl groups, give strong steric interaction and small ligand bite resulting in almost pure low-spin behaviour of the corresponding $Fe(dtc)_3$. Less bulkier substituents (*e.g.* methyl or n-butyl groups) result in spin crossover, while the small steric interference in the pyrrolidinecarbodithiato ligand results in pure high-spin behaviour (Fig. 2).

In the case of tris(4-morpholinecarbodithiato)-iron(III) (FeM) solvates the same variation in magnetic properties as above can be achieved by variation of the solvent molecules present in the crystal lattice (Fig. 3). The low-spin behaviour is obtained by non-polar solvents, *e.g.* benzene and nitrobenzene, and crossover or high-spin behaviour is obtained by polar solvents, *e.g.* dichloromethane, chloroform and water [3].

This paper discusses the influence of the solvent molecules on the magnetic properties of FeM solvates in terms of crystal packing and ligand conformations: the room temperature crystal structure of a novel phase (III) of tris(4-morpholinecarbodithiato)-iron(III) dichloromethane is reported. It is the only known pure high-spin FeM solvate (Phase I at 298 K is described in Ref. 4, while Ref. 5 deals with phase I at 293 and 178 K and phase II at 110 and 20 K).

Experimental

The title compound was prepared by adding morpholine and a 0.1 *M* solution of anhydrous iron(III) chloride in ethanol to a 0.3 *M* solution of sodium hydroxide and carbon disulphide in ethanol. Recrystallization from fresh dichloromethane gave black crystals. Preliminary investigations revealed crystal class 1 with $Z = 2$. The triclinic space group $P\bar{1}$ was indicated by intensity statistics. The single crystal used was tabular (010) bound by {001} and {10$\bar{1}$}.

Unit cell dimensions were determined by least-squares refinement of 27 reflexions with $5° < \theta < 22°$. The reflexions were measured with MoKα radiation on a Enraf-Nonius CAD4 diffractometer. Intensity data were collected in a complete half-sphere of reciprocal space with $3° < \theta < 25°$. A reflexion was considered observable if $I \geqslant 3\sigma_c(I)$ in the pre-scan ($\sigma_c(I)$ is based on counting statistics). Three control reflexions measured every two hours showed no systematic intensity variations. Data were corrected for Lorentz, polarization and absorption effects. Centrosymmetrically related reflexions were averaged before structure solution commenced.

Magnetic susceptibility was measured with a microcomputer-controlled Cahn RG electrobalance using the Faraday principle [6, 7]. Polycrystalline samples were used with field strengths of 0.6 and 0.8 T. Effects from solvent loss were investigated through careful grinding and heating (to ~90 °C) under vacuum to constant weight.

Solution and Refinement of the Structure

The FeS_6 core of the complex was located using MULTAN [8]. Consecutive differential maps gave the positions of all other non-H atoms. The dichloromethane molecule is statistically distributed over two centrosymmetrically related positions near the origin; the occupancy 0.5 was assumed for both. The H-atom positions were calculated from geometric considerations with C–H = 0.90 Å when used in refinements and C–H = 1.05 Å when used in the final distance calculations. Anisotropic temperature factor coefficients were refined for non-H atoms while H atoms were assigned fixed isotropic temperature factor coefficients ~25% greater than the isotropic mean value of the adjacent C atom.

The function $\Sigma w(\Delta F)^2$ was minimized with full matrix least-squares refinement. The weights w were calculated from $w^{-1} = \sigma_c^2(|F_o|) + (c_1|F_o|)^2 + c_2$ with c_1 and c_2 adjusted to give constant $\langle w(\Delta F)^2 \rangle$ in different $|F_o|$ and $\sin(\theta)$ intervals. Only parameters of non-H atoms were refined. The dichloro-

TABLE I. Some Crystal Data, Data Collection and Reduction and Structure Refinement of $Fe[S_2CNC_4H_8O]_3 \cdot CH_2Cl_2$ Phase III.

T (K)	293
a (Å)	9.264(1)
b (Å)	10.459(1)
c (Å)	13.665(2)
α (°)	100.65(1)
β (°)	95.60(1)
γ (°)	105.83(1)
V (Å^3)	1236(1)
D_x (g cm^{-1})	1.684
μ-MoK_α (mm^{-1})	1.34
Crystal size (mm^3)	0.37 × 0.21 × 0.10
Range of transmission factors	0.76–0.87
$\omega-2\theta$ scan width, $\Delta\omega$ (°)	1.0 + 0.5 tanθ
$\sigma_c(I)/I$ requested in scan	0.033
Max. recording time	180
No. of reflexions recorded	4602
considered not observable	1598
in final LS cycle, m	2811
No. of parameters refined, n	280
$R = \Sigma\|\Delta F\|/\Sigma\|F_o\|$	0.028
$R_w = [\Sigma w\|\Delta F\|^2/\Sigma w\|F_o\|^2]^{1/2}$	0.034
$S = [\Sigma w\|\Delta F\|^2/(m-n)]^{1/2}$	0.473
c_1 (in weighting function)	0.03
c_2 (in weighting function)	2.00

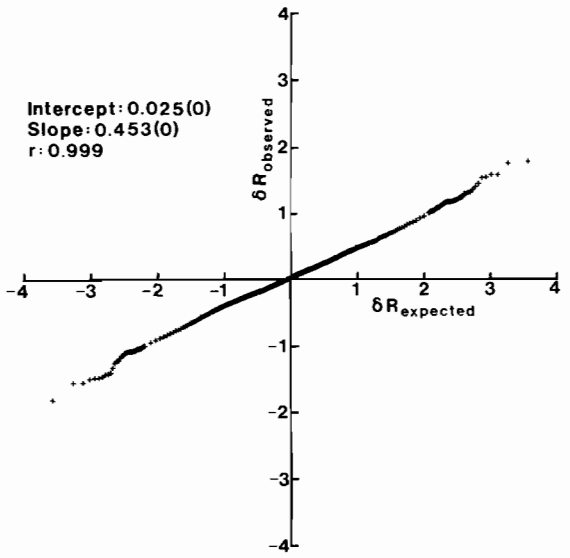

Fig. 4. δR-plot comparison of data and model for $Fe(S_2CNC_4H_8O)_3 \cdot CH_2Cl_2$ phase III.

TABLE II. Atomic Coordinates (×10^4) and Mean Isotropic Temperature Factor Coefficients of non-H Atoms of $[Fe[S_2CNC_4H_8O]_3 \cdot CH_2Cl_2$ Phase III. The occupancy factors for Cl(1), Cl(2) and C is 0.5.

	x/a	y/b	z/c	B_{iso}/Å^2
Fe	3226(1)	3172(1)	6638(1)	3.09(1)
S(1)	5380(1)	2565(1)	6006(1)	3.54(2)
S(2)	3331(1)	1081(1)	7157(1)	3.64(3)
C(1)	4898(4)	1191(3)	6561(2)	3.11(9)
N(1)	5666(3)	291(3)	6524(2)	3.63(9)
C(2)	5183(4)	−964(4)	6896(3)	4.35(12)
C(3)	7192(4)	448(4)	6121(3)	4.02(11)
C(10)	6431(5)	−1056(4)	7622(3)	5.21(14)
C(11)	8276(4)	321(4)	6910(3)	4.78(13)
O(1)	7801(3)	−928(3)	7215(2)	5.45(10)
S(3)	3050(1)	4686(1)	5511(1)	3.93(3)
S(4)	988(1)	2003(1)	5372(1)	3.67(2)
C(4)	1416(4)	3454(3)	4900(2)	2.28(9)
N(2)	533(3)	3618(3)	4145(2)	3.92(9)
C(5)	−876(4)	2587(4)	3608(3)	4.75(12)
C(6)	909(4)	4806(4)	3684(3)	4.59(12)
C(12)	−735(5)	2204(5)	2532(4)	5.61(15)
C(13)	1009(5)	4325(5)	2599(4)	5.91(17)
O(2)	−363(4)	3348(3)	2081(2)	5.93(11)
S(5)	4899(1)	5070(1)	7941(1)	3.86(3)
S(6)	1740(1)	3704(1)	7963(1)	3.97(3)
C(7)	3358(4)	4962(3)	8561(2)	3.49(10)
N(3)	3440(4)	5775(3)	9445(2)	4.40(9)
C(8)	4793(5)	6890(4)	9948(3)	4.80(12)
C(9)	2166(5)	5650(5)	10019(4)	6.11(16)
C(14)	4343(7)	8179(5)	10184(4)	6.90(18)
C(15)	1882(7)	6974(7)	10310(4)	8.36(23)
O(3)	3165(5)	8034(4)	10780(3)	8.12(14)
Cl(1)	1020(9)	1148(9)	−156(8)	15.84(35)
Cl(2)	1328(8)	778(9)	−370(6)	12.14(25)
C	−431(20)	206(28)	−135(19)	14.92(1.12)

methane parameters were refined separately and kept constant in the final LS cycles. The H atom coordinates and isotropic B values were recalculated between every second LS cycle.

The refinements were considered completed when parameter shifts/e.s.d. were below 1%. The final difference map showed some residual peaks of heights <0.5 e Å^3 in the vicinity of the dichloromethane molecule. A probability plotting of ordered values of $\delta R_i = \Delta F_i/\sigma(|F_o|_i)$ *vs.* those expected for ordered deviates ($\sigma(|F_o|_i) = w^{-1/2}$) is shown in Fig. 4. The shape and intercept of the curve indicates very small systematic errors. Further data concerning data collection and reduction and structure refinement are given in Table I.

Atomic scattering factors and dispersion correction factors were taken from [9]. Atomic coordinates and mean isotropic B values are given in Table II. The observed and calculated structure amplitudes

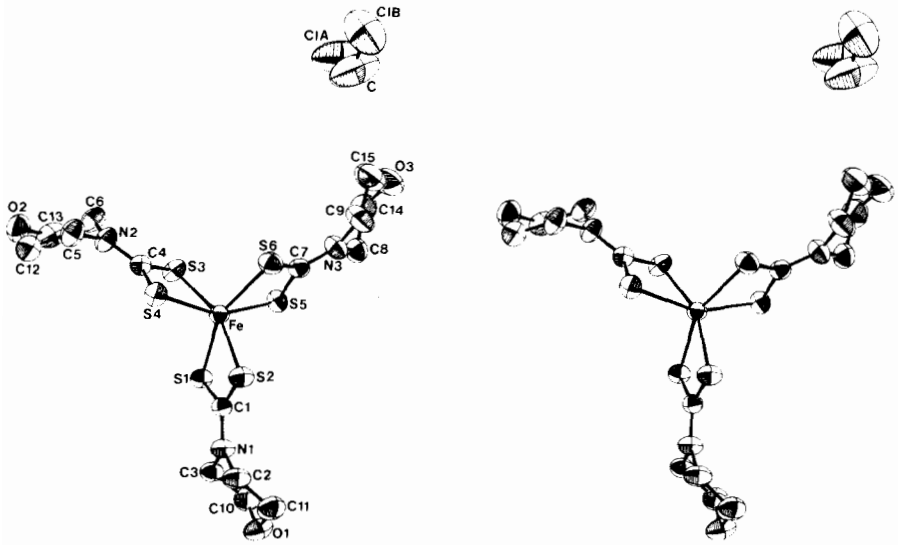

Fig. 5. Stereoscopic drawing of $Fe(S_2CNC_4H_8O)_3 \cdot CH_2Cl_2$ phase III viewed along the pseudo threefold axis. Only one of the CH_2Cl_2 positions is shown. The thermal ellipsoids are scaled to include 50% probability.

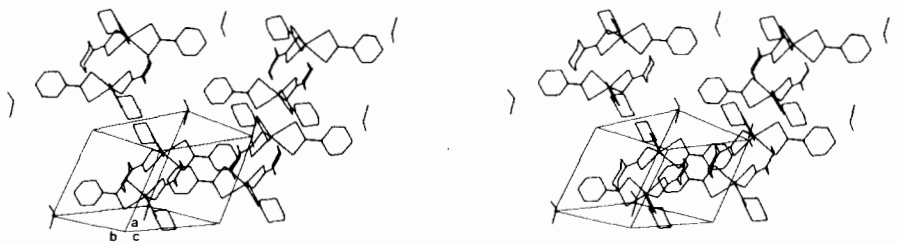

Fig. 6. Stereoscopic drawing of the crystal packing of $Fe(S_2CNC_4H_8O)_3 \cdot CH_2Cl_2$ phase III. Only one of the CH_2Cl_2 positions is shown.

TABLE III. Selected Intramolecular Distances (Å) and Bond Angles (°) in the $Fe[S_2CN(CH_2)_4O]_3$ Complex and the CH_2Cl_2 Solvate Molecule and r.m.s. Deviations (Å) from the Least-Squares Planes through the S_2CNC_2 Groups.

(*a*) the FeS_6 core	
Fe–S(1)	2.441(1)
Fe–S(2)	2.442(1)
Fe–S(3)	2.427(1)
Fe–S(4)	2.433(1)
Fe–S(5)	2.447(1)
Fe–S(6)	2.451(1)
S(1)–S(2)	2.892(1)
S(3)–S(4)	2.890(1)
S(5)–S(6)	2.891(1)
S(1)–S(3)	3.592(1)
S(1)–S(5)	3.515(1)
S(3)–S(5)	3.485(1)
S(2)–S(4)	3.544(1)
S(2)–S(6)	3.507(1)
S(4)–S(6)	3.562(1)
S(1)–Fe–S(2)	72.64(3)
S(3)–Fe–S(4)	72.99(3)
S(5)–Fe–S(6)	72.33(3)
(*b*) Ligand 1	
C(1)–S(1)	1.720(3)
C(1)–S(2)	1.719(3)
S(1)–C(1)–S(2)	114.4(2)
C(1)–N(1)	1.321(4)
N(1)–C(2)	1.467(5)
C(2)–C(10)	1.483(6)
C(10)–O(1)	1.417(5)
O(1)–C(11)	1.413(5)
C(11)–C(3)	1.504(5)

(continued overleaf)

TABLE III. *(continued)*

C(3)–N(1)	1.469(5)
N(1)–C(2)–C(10)	110.2(3)
C(2)–C(10)–O(1)	112.4(4)
C(10)–O(1)–C(11)	110.9(3)
O(1)–C(11)–C(3)	111.8(3)
C(11)–C(3)–N(1)	108.6(3)
C(3)–N(1)–C(2)	112.7(3)
r.m.s. deviation	0.0324
(c) Ligand 2	
C(4)–S(3)	1.714(3)
C(4)–S(4)	1.719(3)
S(3)–C(4)–S(4)	114.7(2)
C(4)–N(2)	1.319(4)
N(2)–C(5)	1.469(5)
C(5)–C(12)	1.478(6)
C(12)–O(2)	1.421(6)
O(2)–C(13)	1.417(6)
C(13)–C(6)	1.495(6)
C(6)–N(2)	1.468(5)
N(2)–C(5)–C(12)	109.2(3)
C(5)–C(12)–O(2)	112.5(4)
C(12)–O(2)–C(13)	111.0(3)
O(2)–C(13)–C(6)	111.4(4)
C(13)–C(6)–N(2)	108.5(3)
C(6)–N(2)–C(5)	111.7(3)
r.m.s. deviation	0.0110
(d) Ligand 3	
C(7)–S(5)	1.718(3)
C(7)–S(6)	1.712(3)
S(5)–C(7)–S(6)	114.8(2)
C(7)–N(3)	1.325(5)
N(3)–C(8)	1.463(5)
C(8)–C(14)	1.505(6)
C(14)–O(3)	1.416(7)
O(3)–C(15)	1.386(7)
C(15)–C(9)	1.468(8)
C(9)–N(3)	1.470(6)
N(3)–C(8)–C(14)	108.2(4)
C(8)–C(14)–O(3)	111.2(4)
C(14)–O(3)–C(15)	112.1(4)
O(3)–C(15)–C(9)	114.1(5)
C(15)–C(9)–N(3)	110.4(4)
C(9)–N(3)–C(8)	113.0(3)
r.m.s. deviation	0.0133
(e) CH_2Cl_2	
C–Cl(1)	1.513(28)
C–Cl(2)	1.661(20)
Cl(1)–C–Cl(2)	122.6(1.5)

and anisotropic temperature factor coefficients are available on request.

TABLE IV. Packing of the Complexes in $Fe[S_2CNC_4H_8O]_3 \cdot CH_2Cl_2$ Phase III. Intermolecular distances (Å) less than 3.8 Å, the shortest distances between CH_2Cl_2 and the complex and the shortest Fe–Fe distances.

The superscripts (i)–(vii) denote the following transformations of the x, y, z values given in Table II:

(i) $1-x, 1-y, 1-z$
(ii) $\bar{x}, \bar{y}, 1-z$
(iii) $1-x, \bar{y}, 1-z$
(iv) $1-x, 1-y, 2-z$
(v) $\bar{x}, y, z$
(vi) $\bar{x}, 1-y, 1-z$
(vii) $\bar{x}, y, \bar{z}$

$S(1)–C(6)^{i}$	3.698(4)
$S(2)–C(5)^{ii}$	3.776(5)
$S(2)–C(12)^{ii}$	3.738(5)
$C(1)–C(3)^{iii}$	3.798(5)
$C(1)–O(3)^{iv}$	3.732(5)
$N(1)–O(3)^{iv}$	3.690(5)
$C(10)–O(3)^{iv}$	3.395(6)
$O(1)–C(12)^{iii}$	3.353(5)
$S(4)–C(11)^{v}$	3.715(4)
$C(4)–C(6)^{vi}$	3.652(5)
$N(2)–N(2)^{vi}$	3.780(6)
$N(2)–C(6)^{vi}$	3.669(5)
$C(13)–S(6)^{vi}$	3.793(5)
$O(2)–S(6)^{vi}$	3.649(3)
$O(2)–C(7)^{vi}$	3.789(5)
$O(2)–N(3)^{vi}$	3.779(4)
$O(2)–C(9)^{vi}$	3.640(6)
$O(2)–C(15)^{vi}$	3.348(6)
$C(7)–C(8)^{iv}$	3.662(5)
$N(3)–C(8)^{iv}$	3.768(5)
$Cl(1)–C(8)^{i}$	3.82(1)
$Cl(2)–C(8)^{i}$	3.67(1)
$Cl(2)–C(12)^{vii}$	3.75(1)
$Cl(2)–C(14)^{i}$	3.83(1)
$C–C(15)^{vi}$	3.59(3)
$C–O(3)^{vi}$	3.64(2)
$C–O(1)^{vii}$	3.66(2)
$C–C(10)^{vii}$	3.78(2)
C–C(12)	3.93(3)
$Fe–Fe^{i}$	6.913(1)
$Fe–Fe^{ii}$	7.868(2)
$Fe–Fe^{iii}$	8.865(1)

Results and Discussion

Description of the Structure

The crystal structure comprises mononuclear complexes with pseudosymmetry D_3 and dichloromethane molecules packed together by van der Waals forces. Figure 5 shows a stereoscopic pair of drawings of the complex and Fig. 6 the packing of the complexes. Selected intramolecular distances and angles are given in Table III with intermolecular distances in Table IV.

TABLE V. Some Mean Geometric Characteristics of the FeS_6 Polyhedron of Tris(4-morpholinecarbodithiato)iron(III) Dichloromethane Phase III (A) Compared to Tris(1-pyrrolidinecarbodithiato)iron(III) [10] (B).

	A	B
μ_{eff} (B.M.)	5.92	5.92
⟨Fe–S⟩ (Å)[a]	2.440(1)	2.456(2)
⟨S–Fe–S⟩ (°)[a]	72.65(3)	72.65(4)
Edge of triangular faces (Å)[a]	3.534(1)	3.564(2)
Height of prism (Å)	2.675(2)	2.680(2)
Trigonal twist (°)[a]	31.1(1)	31.9(1)
Tilt between triangular faces (°)	1(1)	1(1)

[a]Tabulated e.s.d.s are r.m.s. values of the individual e.s.d.s.

The geometry of the three ligands do not differ significantly from each other and is within the range observed in other $Fe(dtc)_3$ compounds. The crystal packing induces a significant scatter in the Fe–S distances, although the ligand bites (the S···S distances) are equal. The mean geometry of the FeS_6 core of the complex is that expected for a pure high-spin $Fe(dtc)_3$ complex (Table V). The dichloromethane molecules are located in the vicinity of the O-ends of ligands 1 and 3, statistically distributed over two centrosymmetrically related positions. The thermal parameters indicate severe disorder. There is no evidence for hydrogen bonding between the complex and the solvent molecule as in phase I and II [5].

Structure-Property Relationships in Tris(4-morpholinecarbodithiato)iron(III) Solvates

The temperature dependence of μ_{eff} for some FeM solvates is shown in Fig. 3. The magnetic properties of the title compound (curve *a* in Fig. 3) were first described in Ref. 15, but were then assigned $FeM{\cdot}CH_2Cl_2$ phase I. The solvent molecules can be divided into two groups according to how they shift the spin state relative the desolvated FeM [3]: (A) non-polar solvents (*e.g.* benzene and nitrobenzene) are located around the relatively non-polar morpholine rings of the ligands and shift μ_{eff} towards lowspin, (B) polar solvents (*e.g.* dichloromethane, chloroform and water) are with the exception of the title compound located near the relatively polar FeS_6 core of the complex and shift μ_{eff} towards high-spin. Obviously the solvent molecules influence the magnetic properties through differences in the crystal packing.

Some geometric characteristics of the morpholinecarbodithiato ligand averaged over the three ligands in a FeM complex are given in Table VI. The conformation of the morpholine rings are given as the puckering parameters θ, ϕ and Q defined by Cremer and Pople [14]. Studies of the morpholine rings are complicated by frequent disorder in the crystal structures, but the average conformations can be described as half-chair or twisted (the dibenzene solvate) and show no significant correlation to μ_{eff}. A deformation parameter γ is defined as the angle between the normals to the S_2C and NC_2 planes, thus accounting for both bending and rotation about the central C–N bond. The parameter γ is strongly correlated to μ_{eff} (Table VI and Fig.

TABLE VI. Some Geometric Characteristics of the Morpholinecarbodithiato Ligand in Tris(4-morpholinecarbodithiato)iron(III) Solvates. Definitions in text. The θ and ϕ values are compared to those of pure chair, boat and twist conformations.

No. (*cf.* Fig. 7)	Solvent molecule	Temperature (K)	Phase no.	μ_{eff} (B.M.)	θ (°)	ϕ (°)	Q	R.m.s. deviation from S_2CNC_2 plane	γ (°)	Original coordinates from ref.
1	CH_2Cl_2	20	II	3.80	43.1(1)	148(2)	1.58(3)	0.0266	10.1	5
2	CH_2Cl_2	110	II	4.45	28.9(4)	147(1)	2.15(2)	0.0221	8.3	5
3	CH_2Cl_2	178	I	5.05	34.4(8)	147(1)	1.70(2)	0.0199	7.4	5
4	CH_2Cl_2	293	I	5.60	28.6(8)	148(1)	1.91(2)	0.0141	5.8	5
5	CH_2Cl_2	293	III	5.92	38.0(3)	147(1)	1.44(1)	0.0189	4.6	This work
6	$CHCl_3$	300		5.45	34.6(2)	147(1)	1.90(1)	0.0213	5.4	11
7	H_2O	300		5.50	22.2(2)	143(3)	1.87(1)	0.0166	4.6	11
8	$C_6H_5NO_2$	300		4.00	27.9(2)	146(1)	2.20(1)	0.0202	10.1	12
9	C_6H_6	300		3.50	58.1(4)	170(1)	1.12(1)	0.1302	9.5	13
	Chair conformation				0	0				
	Boat conformation (n = 0, 1, 2...)				90	n·60				
	Twist conformation (n = 0, 1, 2...)				90	30 + n·60				

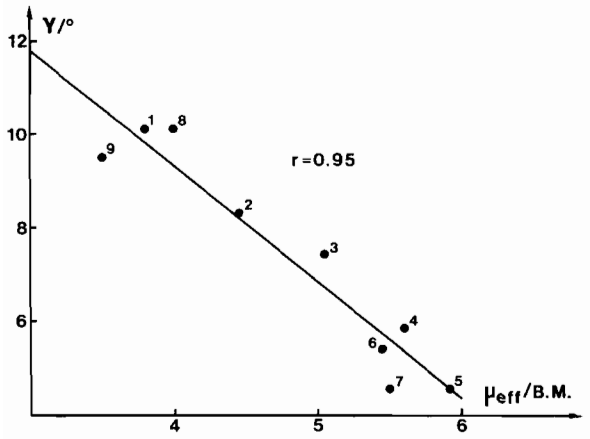

Fig. 7. The ligand distorsion parameter γ *vs.* effective magnetic moment for some tris(4-morpholinecarbodithioato)iron(III) solvates (*cf.* Table VI).

7). The influence of γ on the magnetic properties is seen from the possible canonical forms of a dithiocarbamate ligand (Fig. 8). Canonical form *a* favours the low-spin and form *b* the high-spin state [2]. An increased deformation of the C–N bond will decrease the π-bond overlap in canonical form *b* and instead favour the low-spin form *a*. It is thus concluded that the solvent molecules in FeM solvates influence the magnetic properties through the crystal packing. The differences in the packing forces influence the deformation of the C–N bond in the ligand and thereby its preferred canonical form and consequently the spin state of the Fe(III) ion.

Acknowledgements

I am indepted to Dr. Jörgen Albertsson for many stimulating discussions and Ms Lena Timby for part of the susceptibility measurements and drawing of the illustrations. Financial support from the Royal Physiographic Society in Lund and the Swedish Natural Science Research Council is gratefully acknowledged.

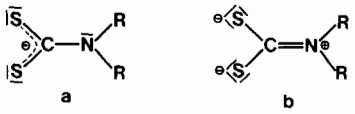

Fig. 8. Proposed canonical forms of the dithiocarbamate ligand.

References

1 A. H. Ewald, R. L. Martin, E. Sinn and A. H. White, *Inorg. Chem., 8,* 1837 (1969).
2 K. Ståhl and I. Ymén, *Acta Chem. Scand.*, in press.
3 E. J. Cukauskas, B. S. Deaver Jr. and E. Sinn, *Inorg. Nucl. Chem. Letters, 13,* 283 (1977).
4 P. C. Healy and E. Sinn, *Inorg. Chem., 14,* 109 (1975).
5 K. Ståhl, *Acta Crystallogr., B39,* in press.
6 J. Albertsson, Å Oskarsson and K. Ståhl, *Acta Chem. Scand., A36,* 783 (1982).
7 B. Blom and T. Hörlin, *Chem. Commun. Univ. Stockholm,* No. 5 (1977).
8 P. Main, S. E. Hull, L. Lessinger, G. Germain, J.-P. Declerq and M. M. Woolfson, *MULTAN, A Program for the Automatic Solution of Crystal Structures from X-Ray Diffraction Data,* Univs. of York, England and Louvain, Belgium (1978);
M. M. Woolfson, *Acta Crystallogr., A33,* 219 (1977).
9 International Tables for X-Ray Crystallography, Kynoch Press, Birmingham, Vol. 4 (1974).
10 S. Mitra, C. L. Raston and A. H. White, *Aust. J. Chem., 31,* 547 (1978).
11 R. J. Butcher and E. Sinn, *J. Am. Chem. Soc., 98,* 5159 (1976).
12 R. J. Butcher and E. Sinn, *J. Am. Chem. Soc., 98,* 2440 (1976).
13 E. J. Cukauskas, B. S. Deaver Jr. and E. Sinn, *J. Chem. Phys., 67,* 1257 (1977).
14 D. Cremer and J. A. Pople, *J. Am. Chem. Soc., 97,* 1354 (1975).
15 A. Malliaris and V. Papaefthimiou, *Inorg. Chem., 21,* 770 (1982).